Vortex Shedding as a Precursor of Turbulent Electrical Activity in Cardiac Muscle

Cándido Cabo, Arkady M. Pertsov, Jorge M. Davidenko, William T. Baxter, Richard A. Gray, and José Jalife
Department of Pharmacology, SUNY Health Science Center at Syracuse, Syracuse, New York 13210 USA

ABSTRACT In cardiac tissue, during partial blockade of the membrane sodium channels, or at high frequencies of excitation, inexcitable obstacles with sharp edges may destabilize the propagation of electrical excitation waves, causing the formation of self-sustained vortices and turbulent cardiac electrical activity. The formation of such vortices, which visually resembles vortex shedding in hydrodynamic turbulent flows, was observed in sheep epicardial tissue using voltage-sensitive dyes in combination with video-imaging techniques. Vortex shedding is a potential mechanism leading to the spontaneous initiation of uncontrolled high-frequency excitation of the heart.

INTRODUCTION

The rhythmic contraction of the heart is triggered by electrochemical waves of excitation that originate in the sinus node and propagate through the atria and ventricles. Multiple anatomical obstacles that are present in the normal heart (e.g., orifices of the caval veins, aorta, pulmonary artery, and coronary arteries perfusing the myocardial wall) normally do not affect the stable propagation of such waves over wide parameter ranges. Here we demonstrate that, under certain critical conditions, inexcitable obstacles may destabilize propagation, causing the formation of self-sustained vortices and uncontrolled high-frequency excitation of cardiac tissue. The formation of such vortices, which visually resembles vortex shedding in hydrodynamical systems (Tritton, 1977), was observed in thin slices of sheep ventricular epicardial muscle using a voltage-sensitive probe in combination with video-imaging techniques (Davidenko et al., 1992). The parameter range for instability was estimated numerically with an ionic model of cardiac muscle (Luo and Rudy, 1991). Instabilities were observed after 75% blockade of sodium channel conductance and at high frequencies of excitation (close to the propagation limit). Wavefront instabilities resulting from interaction with impermeable barriers have been reported previously for generic numerical models of excitable media (Panfilov and Pertsov, 1982; Pertsov et al., 1990; Mikhailov, 1990; Winfree, 1989; Panfilov and Keener, 1993; Agladze et al., 1994; Starobin et al., 1995) and observed experimentally in chemically excitable media (Agladze et al., 1984, 1994; Nagy-Ungvarai et al., 1992; Markus et al., 1994; Zhabotinsky et al., 1993; Toth et al., 1994; Graham et al., 1994). Here we provide the first experimental demonstration of such instabilities in a biological system.

MATERIALS AND METHODS

Computer simulations

To simulate wave propagation in cardiac tissue we used a two-dimensional cable model with Luo and Rudy (1991) kinetics:

$$I_m = \left(\frac{1}{S_v R_{ix}}\right)(V_m)_{xx} + \left(\frac{1}{S_v R_{iy}}\right)(V_m)_{yy} = C_m(V_m)_t + I_{ion},$$

where I_m is the total transmembrane current ($\mu A/cm^2$), S_v is the surface-to-volume ratio (2000 cm^{-1}), R_{ix} is the intracellular resistivity in the x (longitudinal) direction (0.5 kΩ cm), R_{iy} is the intracellular resistivity in the y (transverse) direction (4.5 kΩ cm), V_m is the transmembrane potential, I_{ion} is the total ionic membrane current ($\mu A/cm^2$; Luo-Rudy equations), and C_m is the membrane capacitance (1 $\mu F/cm^2$). The directional difference in intracellular resistivity was imposed to match the anisotropy of myocardial tissue (i.e., directional dependency of the propagation velocity). An inexcitable obstacle was simulated by electrically uncoupling nodes at both sides of a barrier (non-flow boundary conditions at the barrier). To integrate the two-dimensional cable equation, an explicit forward Euler scheme was used with a spatial discretization step of 25 μm and a time integration step of 2 μs. The array consisted of 600 × 300 nodes in the x and y directions, respectively. Non-flux boundary conditions were applied at the boundary of the domain.

Experimental preparations

Young sheep weighing 15 to 25 kg were anesthetized with sodium pentobarbital. The chest was opened through an anterior midline incision, and the heart was excised and placed in warm oxygenated Tyrode's solution. Thin slices (thickness 0.5 mm) of ventricular epicardial muscle were cut with a dermatome. Suitable preparations of about 20 mm by 20 mm were placed in a recording chamber and superfused with oxygenated Tyrode's solution (37°C) containing diacetyl-monoxime (15 mM) to abolish contractility. Tissues were stained with the fluorescent voltage-sensitive probe DI-4-ANEPPS (15 μM; Molecular Probes, Eugene, OR). Video-imaging techniques (Davidenko et al., 1992) were used to record the excitation waves as fluorescence changes proportional to changes in transmembrane potential. Fluorescence was excited at 490 nm and recorded at 645 nm with a CCD video camera (Cohu series 6500) at a rate of 60 frames/s. The images of an area of approximately 20 × 20 mm (400 × 200 pixels) were acquired for 1–2 s by a 16-Mbyte video board (dynamic range, 8 bits) connected to a Pentium PC and stored on an optical disc. To extract the

Received for publication 25 May 1995 and in final form 12 December 1995.

Address reprint requests to Dr. Arkady Pertsov, Department of Pharmacology, SUNY Health Science Center, 766 Irving Avenue, Syracuse, NY 13210. Tel.: 315-464-7949; Fax: 315-464-8000; E-mail: pertsov@sunbird.pharm.hscsyr.edu.

0006-3495/96/03/1105/07 $2.00

voltage-dependent signal, digital subtraction of the background fluorescence (prefiltering spatial resolution 100 μm) and spatial filtering were performed (conical filter with a radius of 4 pixels, post-filtering spatial resolution 400 μm).

An inexcitable barrier was created by making a linear cut perpendicular to one of the borders of the tissue slice using fine scissors. A healing-over period of half an hour was allowed after the cut was made. From histological and immunocytochemical studies it was estimated that the extent of damaged cells beyond the cut was about 100 μm (Cabo et al., 1994). Therefore, the barrier can be considered a sharp corner because its radius (100 μm) is smaller than other relevant dimensions (wave front width 0.5–1 mm). Excitation waves were initiated by electrical stimulation delivered through Ag-AgCl electrodes (diameter, 0.2 mm) with an amplitude three times the threshold value. In addition to the optical recordings, transmembrane potentials were continuously recorded using glass microelectrodes filled with 3 M KCl and connected to a microprobe system (model 705; World Precision Instruments, New Haven, CT).

The effect of the barrier on propagation was studied at normal excitability during superfusion of the slices of epicardial tissue with Tyrode's solution (control) and at low excitability (5 experiments) by adding the sodium channel blocker tetrodotoxin (TTX) (15 μM) to the perfusate. The optical recordings were made before TTX superfusion (control), 5 min after initiation of the TTX superfusion for a period of 30 min, and 15 min after the initiation of the wash-out. Ten experiments were performed to study the effects of the barrier on propagation at various interstimulus intervals in preparations superfused with normal Tyrode's solution (normal excitability). Stimulation was applied to the tissue using trains of 10–15 stimuli at interstimulus intervals that ranged between 500 ms (control) and the shortest interval that resulted in 1:1 propagation. The changes in critical radius for propagation with interstimulus interval were estimated in seven additional experiments using the method described below.

Relevant parameters

To relate the mechanism of the instabilities observed in myocardial tissue to similar instabilities in other excitable media, the critical ratio R_{cr}/W (Pertsov et al., 1983) was estimated both computationally and experimentally. Here R_{cr} is the critical radius for excitation and W is the width of the wave front. R_{cr} characterizes the minimum area that has to be excited to initiate a propagating wave and is similar to the liminal length (Rushton, 1937), but for a two-dimensional excitable medium. In computer simulations, R_{cr} was measured after removing the anisotropy of the medium by rescaling the governing two-dimensional cable equation (i.e., in an isotropic medium). R_{cr} was defined as the minimum radius, such that depolarization to 30 mV of a circle with such a radius resulted in a propagating wave (Cabo et al., 1994). The width of the wave front, W, was defined as the spatial extent of tissue having an inward sodium current during propagation of a planar wave.

Experimentally, R_{cr} was estimated indirectly from measurements of the critical width of an isthmus. Computer simulations show that such an estimate is in good agreement with the measurements of R_{cr} described above. For details on the experimental protocol see Cabo et al. (1994). Briefly, the width of the isthmus was gradually decreased until propagation through it failed. The minimum width of the isthmus (d) sufficient for propagation was used as an estimate of R_{cr} ($R_{cr} = d/2$). The frequency dependence of R_{cr} was estimated ($n = 7$) by measuring the critical frequency (i.e., the frequency of stimulation at which propagation through the isthmus failed) for varying widths of the isthmus. The isthmus was oriented perpendicular to fiber orientation.

The width of the wave front W was estimated indirectly by multiplying the duration of the action potential upstroke derived from microelectrode recordings and the velocity of propagation derived from the optical recordings. Upstroke duration was estimated at 10% to 90% of the amplitude. Validation of measurements of conduction velocity from the optical recordings is given elsewhere (Cabo et al., 1994). As stated above, during our measurements of R_{cr}, the isthmus was usually oriented perpendicular to the fiber orientation. Accordingly, to obtain R_{cr}/W independently of anisotropy, W was estimated for transverse propagation.

RESULTS

In Fig. 1, we present examples of stable propagation during the diffraction of an excitation wave at the edge of a barrier in a computer simulation (Fig. 1 *a*) and an experimental preparation of isolated cardiac tissue (Fig. 1 *b*). In each case, a wave initiated by electrical stimulation beneath the barrier propagated from left to right. The horizontal velocity of propagation (longitudinal to fiber orientation) was 0.40 m/s, and the vertical velocity (transverse to fiber orientation) was 0.12 m/s. Such values are typical of our experimental preparations (longitudinal velocity, 0.38 ± 0.07 m/s, $n = 7$; transverse velocity 0.095 ± 0.026 m/s, $n = 7$). As a consequence of the anisotropy, the wave had an elliptical shape and different wavefront widths in the longitudinal and transverse directions. After initiation, the wave circumnavigated the barrier (yellow) without detaching from it or from the boundary of the domain, and proceeded to excite the medium behind the barrier (no "shadow"). Such a pattern is characteristic of excitable media (Pertsov et al., 1990; Panfilov and Keener, 1993; Agladze et al., 1994; Zhabotinsky et al., 1993; Toth et al., 1994; Graham et al., 1994; Cabo et al., 1994) but is very different from wave

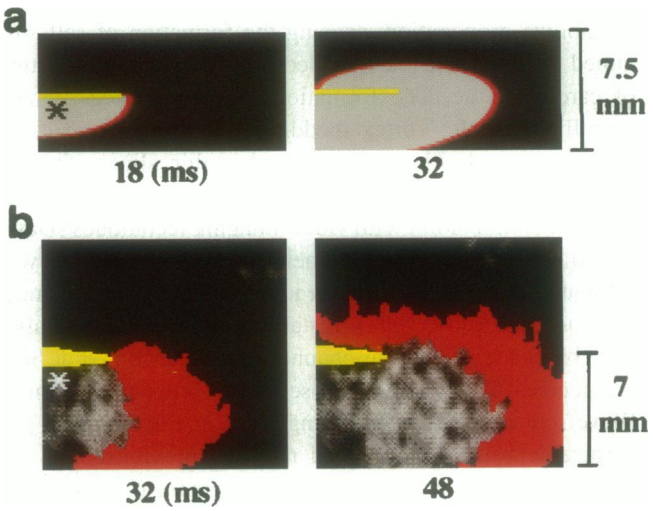

FIGURE 1 Diffraction of excitation waves at the edge of an impermeable barrier in a computer model (*a*) and in a thin slice of sheep epicardial tissue (*b*). In each panel, two sequential snapshots are presented. The wave front is shown in red. Gray levels show relative values of transmembrane potential (*white*, maximal depolarization; *black*, resting potential). An impermeable barrier is shown in yellow. In the computer simulations, the wave was initiated by depolarizing an area with a radius of 1.25 mm to 30 mV (*asterisk*). In the experiments, the wave was initiated by electrical stimulation at the place indicated by the asterisk with a frequency of 2.4 Hz. Numbers below each frame indicate the time after application of the stimulus. In both computer and biological experiments, a propagating wave turns around the edge of the barrier, with the wave front remaining attached to the boundary. The wave front shown in *a* represents the spatial extent of tissue with an inward sodium current. The wave front shown in *b* was obtained as the difference between of two sequential snapshots of activity and represents the displacement of the wave front during the last 16 ms. To detect the edge of the wave front at each frame, a pixel was considered "depolarized" if its optical signal was above 50% of its maximum value.

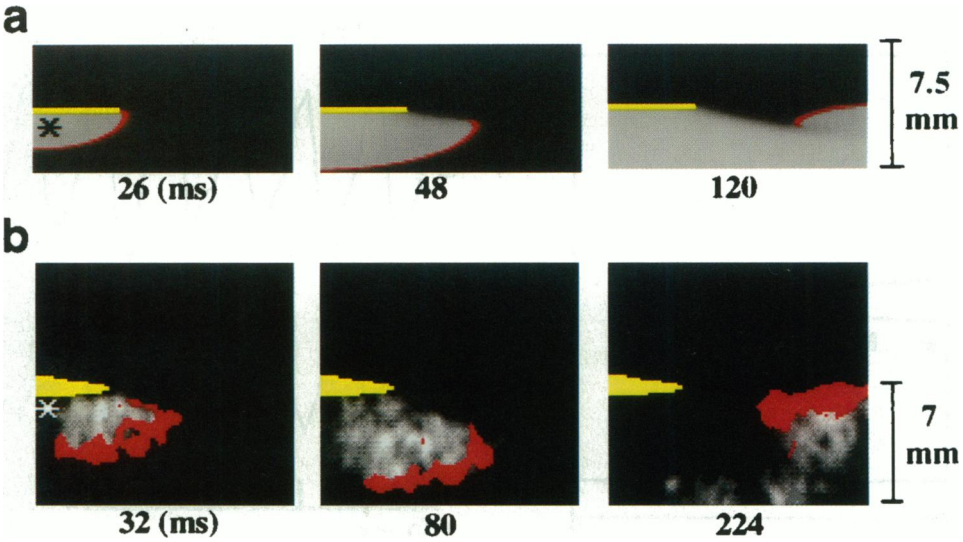

FIGURE 2 Detachment of the wavefront from the edge of a barrier (precursor of turbulence) at a reduced maximum sodium conductance (gNa). Notations are the same as in Fig 1. (*a*) Computer model: gNa was reduced to 25% the value in Fig. 1 *a*. The wave was initiated by depolarizing an area having a radius of 1.25 mm to 30 mV. (*b*) Epicardial tissue: gNa was reduced by perfusion with the sodium channel blocker tetrodotoxin (TTX, 15 μM).

diffraction in conservative systems where the barrier creates a "shadow."

The development of instabilities in both computer and biological experiments is illustrated in Fig. 2. The same experimental protocol as that in Fig. 1 was repeated in the same preparation after reduction of excitability by Na channel blockade. In the model, this was accomplished by reducing maximum sodium conductance (gNa) to 25% of the nominal value; in the experiment, a similar effect was achieved by superfusion with 15 μM TTX. The diffraction pattern changed dramatically. After reaching the edge, the wavefront detached from the barrier and formed a vortex in a manner visually similar (although by a different mechanism) to the separation of the main stream from a body in hydrodynamical systems, where there is subsequent eddy formation during turbulence (Tritton, 1977). The detachment occurred at 26 ms in the computer simulations (Fig. 2 *a*) and at 32 ms in the experiments (Fig. 2 *b*). After losing contact with the barrier the free end of the wave front moved at an angle down toward the lower boundary and made a turn near the right border. The maximum separation of the wavefront from the barrier was about 5–6 mm and could be reliably detected experimentally. After TTX washout, wavefront detachment was reversed and the dynamics expected for the normal tissue were restored.

In the computer simulations, a further decrease in sodium conductance to $\leq$22% normal resulted in shrinking of the wavefront and subsequent annihilation of the wave without vortex formation (Fig. 3). A similar effect has been reported for chemically excitable media (Nagy-Ungvarai et al., 1992). In cardiac tissue the parameter range for the occurrence of this phenomenon is very narrow (there is no propagation at <20% normal gNa). Experimental detachment of the wavefront and subsequent annihilation were observed using TTX superfusion, when the preparation was stimulated at intervals close to the refractory period. (High frequency forcing prevents complete recovery of the Na channels from previous excitation, thus allowing for very fine tuning of gNa.)

Overall, the values of gNa at which detachment was observed in computer simulations (20–30% normal gNa; see Fig. 6 *a*) were consistent with our TTX experiments. Indeed, our estimates indicate that 15 μM TTX reduced the sodium conductance to approximately 32 $\pm$ 5% (n = 4) of the normal value. Such estimates were based on the assumption (Cohen et al., 1984) that action potential upstroke velocity obtained using conventional microelectrode techniques is proportional to gNa.

Detachment and vortex formation could also be observed during high-frequency electrical stimulation, close to the

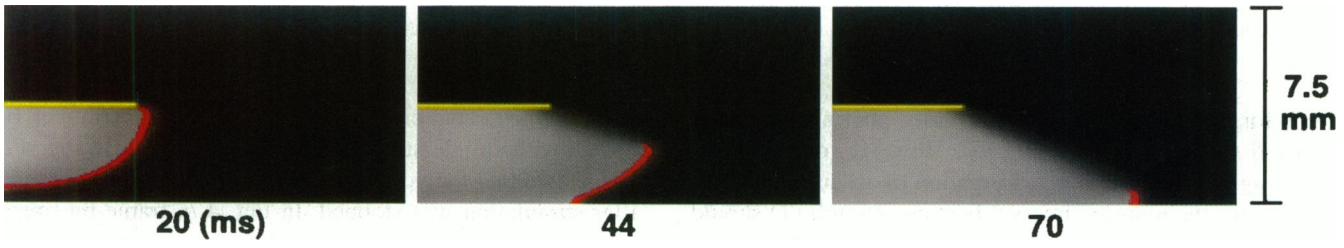

FIGURE 3 Annihilation of a propagating wave after the detachment of the wavefront from the edge of the barrier in the computer model. The maximum sodium conductance (gNa) was reduced to 22% the normal value (Fig. 1 *a*). The wave was initiated by depolarizing an area with a radius of 2.5 mm to 30 mV. Notations are the same as in Fig. 1.

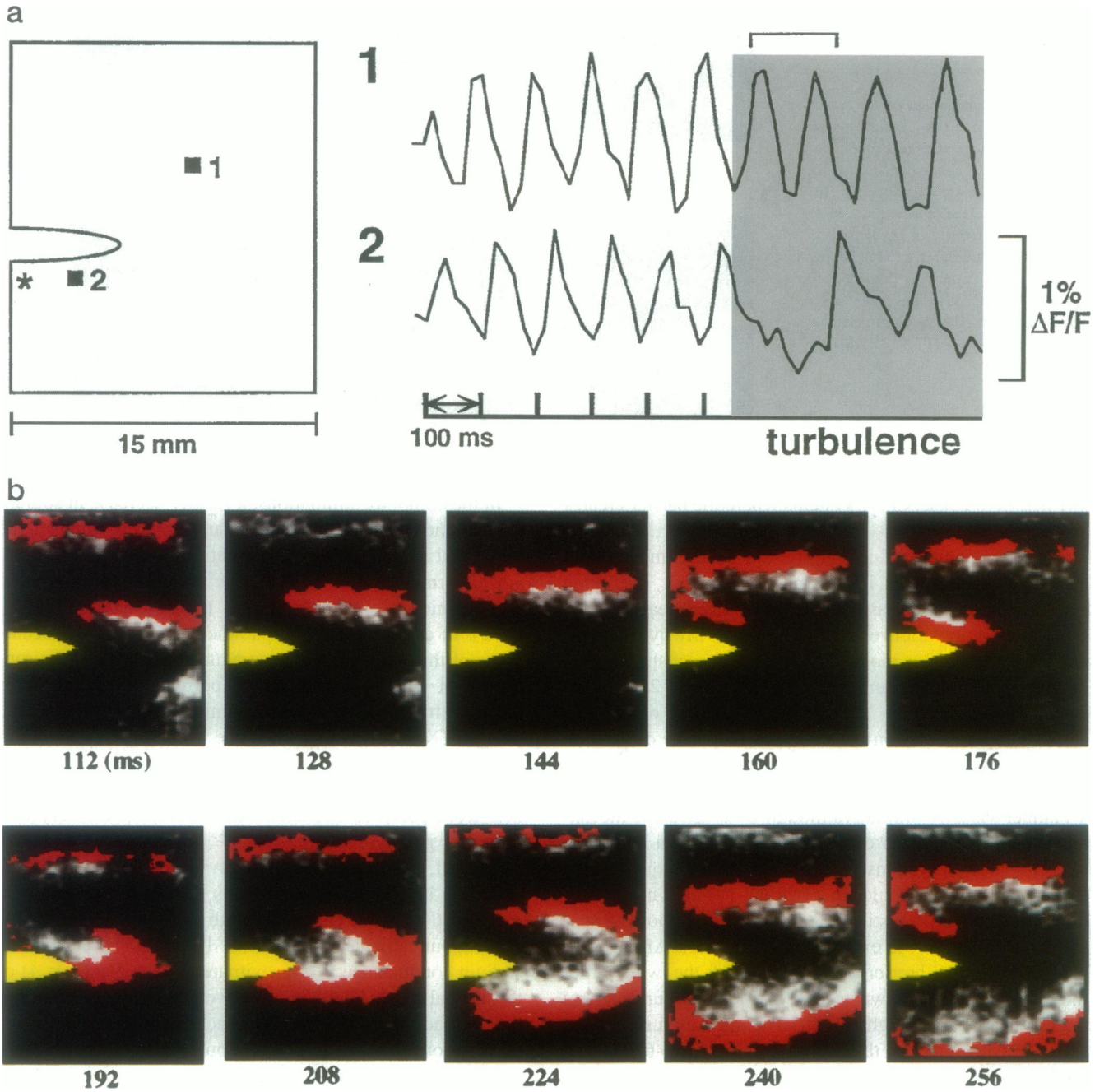

FIGURE 4 Formation of a vortex as a result of high-frequency stimulation after detachment from the edge of the barrier. (*a*) Time course of fluorescence changes at two points located in front of and behind the barrier (*2* and *1*). A train of 10 stimuli with a frequency of 10 Hz was applied at the site indicated by the asterisk. Tics show time of stimulation. Bar indicates time of recording in *b*. The shadowed region represents the time of uncontrolled electrical activity caused by the vortex in the absence of external stimulation. (*b*) Illustration of how the detached wave (last stimulated beat) curled and developed a counterclockwise rotating spiral wave. Notations are the same as in Fig. 1. Numbers under each frame indicate time after the last stimulus of the train.

limit for 1:1 propagation, without any pharmacologically induced sodium channel blockade. However, our observations suggest that, for vortex formation to occur under these conditions, the required interval between stimuli (T) should not exceed by more than 10% (T_{min} = 104 ± 11 ms, T = 114 ± 16 ms, n = 10) the minimum possible interval between propagating waves determined by the recovery time of the tissue (refractory period, T_{min}). In Fig. 4 we illustrate the formation of a vortex as a result of a train of 10 stimuli with an interstimulus interval of 100 ms. In Fig. 4 *a* it is shown that the vortex persisted for an appreciable time after stimulation was stopped. In Fig. 4 *b*, frame-by-frame analysis shows the detachment of the wavefront from the edge of the barrier and subsequent vortex formation. In this case, the vortex developed 160 ms after the last stimulus in the train. Note that wavefronts initiated by the rotating

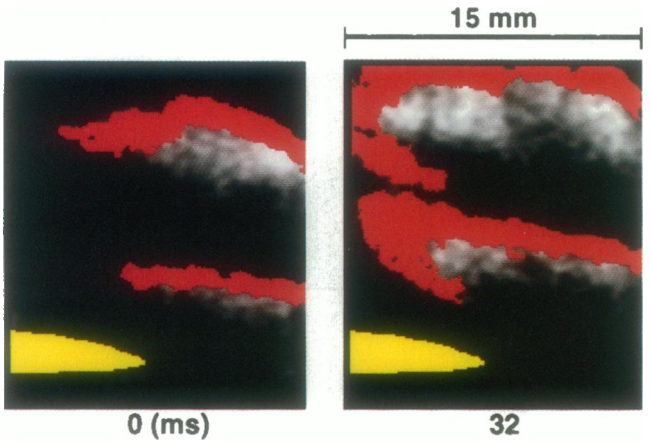

FIGURE 5 Formation of a "vortex street" behind the barrier as a result of sequential detachment of the waves from the edge of the barrier. Notations are the same as in Fig. 1. The snapshots illustrate the formation of a pair of vortices during high-frequency stimulation (8.33 Hz). Propagation is from the bottom to the top.

vortex do not detach from the barrier (frames 176–192 ms). This is a consequence of the fact that the period of rotation of the spiral (140 ± 19 ms, $n = 10$) is larger than the period of the external stimulation (114 ± 16 ms, $n = 10$) required for its initiation. A similar pattern was observed in all nine of the other experiments in which spirals were formed behind the barrier. This is in good agreement with similar experiments in chemically excitable media (Agladze et al., 1994).

The sequential detachment of waves from the barrier during high-frequency stimulation resulted in a pattern similar to vortex shedding in hydrodynamics. Fig. 5 illustrates two counterclockwise vortices formed behind the barrier (propagation is from bottom to top) during stimulation at an interstimulus interval of 120 ms. Such a pattern visually resembles the so-called vortex street that is established behind a cylinder immersed in a fluid (Tritton, 1977) during flows with critical values of the Reynolds' number. However, it should be pointed out that, despite their similarities, the underlying mechanisms responsible for the patterns observed during "turbulence" in excitable media and hydrodynamics are completely different from each other.

We found that, similar to experimental observations in chemically excitable media (Nagy-Ungvarai et al., 1992), in cardiac tissue the detachment and "turbulent" activity correlated with an increase in the ratio R_{cr}/W (see Methods for definitions). Specifically, detachment and turbulence occurred at R_{cr}/W close to or greater than 1. In Fig. 6 *a* we have plotted R_{cr}/W as a function of gNa as calculated in the computer simulations. At normal gNa (100%), R_{cr}/W was less than 1. The plot shows a sharp increase in R_{cr}/W when gNa approaches 35% of the normal value. R_{cr}/W became greater than 1 between 20% and 30% of the normal value of gNa. This was the range where detachment was observed computationally, which agrees with the observations with other excitable media (Pertsov et al., 1983). A similar correlation between R_{cr}/W and vortex shedding was observed in the experimental preparations at high stimulation frequencies (Fig. 6 *b*). R_{cr}/W became greater than 1 at interstimulus intervals shorter than 150 ms, which was close to

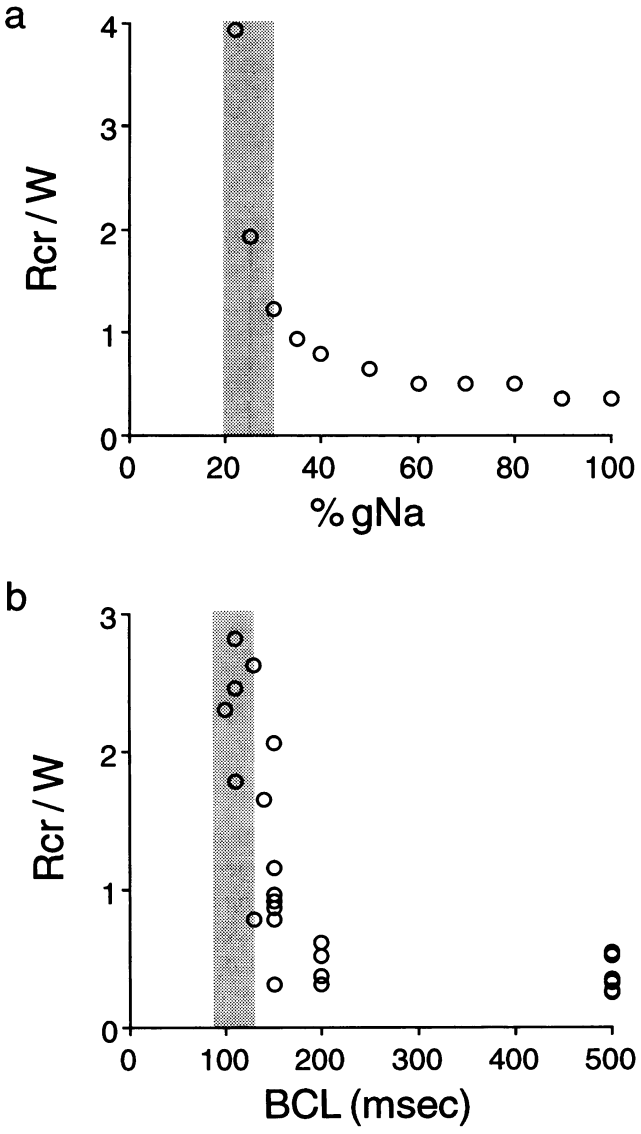

FIGURE 6 Parameter range for detachment and vortex shedding. (*a*) Ratio of the critical radius (R_{cr}) and the width of the wave front (W) as a function of gNa (computer simulations). Detachment occurred when $R_{cr}/W > 1$ (*shaded area*). The lower limit for planar propagation was 18% gNa. For a given gNa, R_{cr} was measured in a continuous (no barrier) isotropic medium as the minimum radius such that depolarization of a circle with that radius to 30 mV resulted in a propagating wave. W is the spatial extent of tissue with an inward sodium current at a certain time. W had a value of 0.4 mm, which did not change with gNa. The values of gNa at which detachment occurred were independent of the anisotropic ratio. (*b*) Illustration of the values of R_{cr}/W obtained for different interstimulus intervals. The values of R_{cr} (cumulative results of seven experiments) were normalized to the mean value of W (0.64 ± 0.18 mm, $n = 16$) obtained at different interstimulus intervals in two experiments. W did not change significantly for different interstimulus intervals (see Discussion). The shaded area corresponds to the range of interstimulus intervals (90–130 ms) at which voxtex shedding occurred (10 experiments).

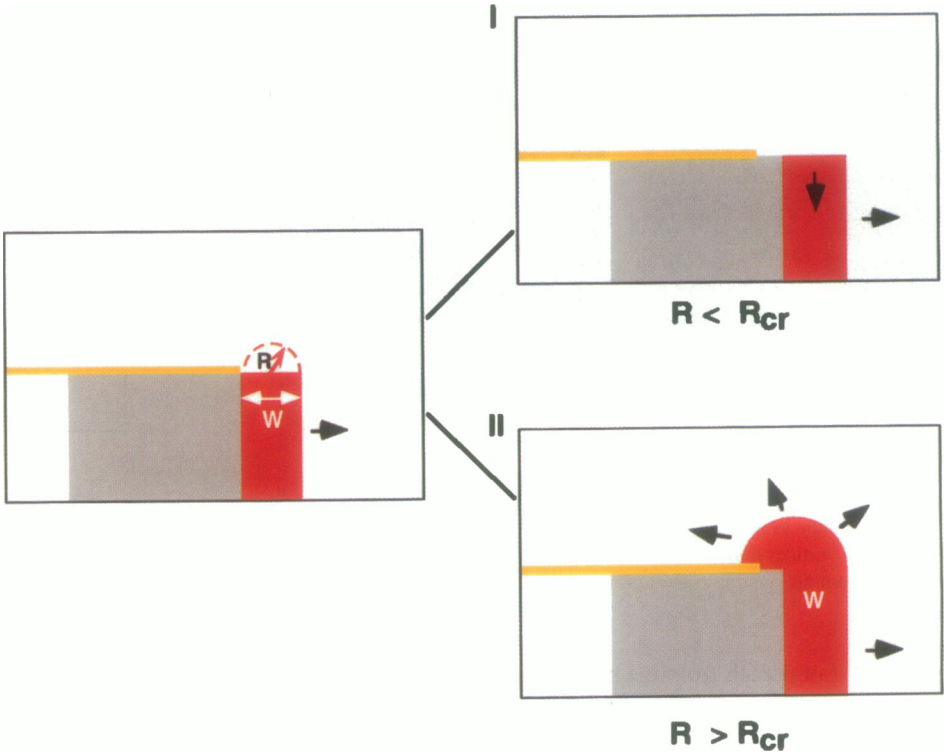

FIGURE 7 Shematic showing the mechanism of detachment. Left panel shows the wave at the time when the wavefront (*red*) reaches the edge of the obstacle (*yellow*). Right two panels show different scenarios for wavefront evolution depending on R_{cr}/W values. See text for explanation.

the interstimulus intervals (90–130 ms) at which vortex shedding was observed. High-frequency forcing causes a reduction in excitability by preventing complete recovery of the Na channels from previous excitation. Our computer simulations show that the critical R_{cr}/W value remained unchanged independently of obstacle orientation in relation to fiber orientation. For a continuous anisotropic cable model this result can be proved analytically by rescaling the model.

DISCUSSION

Our data show that during partial blockade of the membrane sodium channels or at high frequencies of excitation, inexcitable obstacles with sharp edges may destabilize the propagation of the excitation waves in cardiac tissue. This may lead to the formation of self-sustained vortices and turbulent electrical activity.

The mechanism of this phenomenon may be explained as depicted in the scheme shown in Fig. 7. For simplicity, here we consider an isotropic case. The left panel shows an excitation wavefront that just moved beyond the right edge of the obstacle. The dashed curve bounds the area adjacent to the obstacle, which receives lateral current. The radius of this area R is comparable to the width of the wavefront W. If R is smaller than the minimum radius of excitation R_{cr} for a given tissue ($R_{cr}/R < 1$), the wavefront will be unable to progress laterally (upward) or to make a turn. Eventually, the wavefront will detach from the edge of the obstacle, as shown in the upper right panel. If $R_{cr}/R > 1$ (*lower right panel*), the front will progress upward without detachment. Note that substituting R for W in the denominator of the above inequality yields the R_{cr}/W ratio. This explains the correlation of the detachment with the increase in the dimensionless ratio R_{cr}/W. It should be noted, however, that R_{cr}/W is just an empirical dimensionless parameter and, to date, there is no quantitative theory relating R_{cr}/W to separation of the wavefront from the obstacle.

Similar to chemically excitable media, an increase in R_{cr}/W and detachment of the wavefront from the obstacle are related to decreased excitability (see Fig. 6). Indeed, it is qualitatively clear that at lower excitability R_{cr} must increase (the minimum area that has to be excited to initiate a propagating wave increases). In contrast, W (the product of propagation velocity and the duration of the upstroke) should not change significantly; an increase in the upstroke duration at low excitability is compensated for by a reduction in the propagation velocity. As a result, the ratio R_{cr}/W has to increase.

From our data it is clear that detachment of the wavefront from the edge of the obstacle need not result in spiral wave formation, for two important reasons. First, the free end does not always curl (see Fig. 3). Second, the free end does not always separate far enough from the obstacle. Sufficient separation is essential for enabling a full turn without reattachment to the obstacle. In fact, spiral wave formation requires that the maximum separation should be comparable to one wavelength of a spiral wave for a given medium. It is therefore not surprising that separation resulting from reduced gNa does not lead to the same results as separation induced by high-frequency stimulation. Indeed, because high-frequency stimulation is expected to result in greater

abbreviation of action potential duration and wavelength than gNa decrease, separation resulting from high-frequency stimulation would be expected to yield spiral waves more frequently than that resulting from gNa decrease.

The demonstration in myocardial tissue of wave instabilities that are similar to those described in generic models of excitable media and in autocatalytic chemical reactions, and that resemble patterns of hydrodynamical turbulent flow, is much more than just an interesting illustration of the universality of nature. Turbulent propagation and formation of vortices in the heart are thought to be a cause of arrhythmias and sudden cardiac death (Moe and Abildskov, 1959; Krinsky, 1984; Winfree, 1994). Vortex shedding indicates a possible mechanism for the spontaneous initiation of these arrhythmias. We hypothesize that inexcitable thin sclerotic patches and fibrotic tissue, commonly found in elderly patients and diseased heart (Janse and Wit, 1989), provide an appropriate substrate for vortex formation by the interaction of electrical wavefronts with obstacles.

We thank Drs. Jacques Beaumont, Mario Delmar, James P. Keener, Michael Vinson, and Arthur T. Winfree for carefully reading the manuscript and offering helpful suggestions, and JoAnne G. Getchonis and Jiang Jiang for technical assistance.

This work was supported by the National Institutes of Health and the American Heart Association.

REFERENCES

Agladze, K., J. P. Keener, S. C. Muller, and A. Panfilov. 1994. Rotating spiral waves created by geometry. *Science.* 264:1746–1748.

Agladze, K., V. I. Krinsky, and A. M. Pertsov. 1984. Chaos in the non-stirred Belousov-Zhabotinsky reaction is induced by interaction of waves and stationary dissipative structures. *Nature.* 308:834–835.

Cabo, C., A. M. Pertsov, W. T. Baxter, J. M. Davidenko, R. A. Gray, and J. Jalife. 1994. Wave-front curvature as a cause of slow conduction and block in isolated cardiac muscle. *Circ. Res.* 75:1014–1028.

Cohen, C. J., B. P. Bean, and R. W. Tsien. 1984. Maximal upstroke velocity as an index of available sodium conductance. Comparison of maximal upstroke velocity and voltage clamp measurements of sodium current in rabbit Purkinje fibers. *Circ. Res.* 54:636–651.

Davidenko, J. M., A. M. Pertsov, R. Salomonsz, W. Baxter, and J. Jalife. 1992. Stationary and drifting spiral waves of excitation in isolated cardiac muscle. *Nature.* 355:349–351.

Foerster, P., S. C. Muller, and B. Hess. 1988. Curvature and propagation velocity of chemical waves. *Science.* 241:685–687.

Graham, M. D., I. G. Kevrekidis, K. Asakura, J. Lauterbach, K. Krischer, H.-H. Rotermund, and G. Ertl. 1994. Effects of boundaries on pattern formation: catalytic oxidation of CO on platinum. *Science.* 264:80–82.

Janse, M. J., and A. L. Wit. 1989. Electrophysiological mechanisms of ventricular arrhythmias resulting from myocardial ischemia and infarction. *Physiol. Rev.* 69:1049–1169.

Keener, J. P. 1991. An eikonal-curvature equation for action potential propagation in myocardium. *J. Math. Biol.* 29:629–651.

Krinsky, V. I. 1984. Self-Organization: Autowaves and Structures Far from Equilibrium. Springer, Berlin.

Luo, C.-H., and Y. Rudy. 1991. A model of the ventricular cardiac action potential: depolarization, repolarization, and their interaction. *Circ. Res.* 68:1501–1526.

Markus, M., G. Kloss, and I. Kusch. 1994. Disordered waves in a homogeneous, motionless excitable medium. *Nature.* 371:402–404.

Mikhailov, A. S. 1990. Foundations of Synergetics I. Springer, Berlin.

Moe, G. K., and J. A. Abildskov. 1959. Atrial fibrillation as a self-sustaining arrhythmia independent of focal discharge. *Am. Heart J.* 58:59–70.

Nagy-Ungvarai, Z., A. M. Pertsov, B. Hess, and S. C. Muller. 1992. Lateral instabilities of a wavefront in the Ce-catalized Belousov-Zhabotinsky reaction. *Phys. D.* 61:205–212.

Panfilov, A., and J. P. Keener. 1993. Effects of high frequency stimulation on cardiac tissue with an inexcitable obstacle. *J. Theor. Biol.* 163: 439–448.

Panfilov, A., and A. M. Pertsov. 1982. Mechanism of spiral wave initiation in active media connected with critical curvature phenomenon. *Biofizika.* 27:868–888.

Pertsov, A. M., E. A. Ermakova, and E. E. Shnol. 1990. On the diffraction of autowaves. *Phys. D.* 44:178–190.

Pertsov, A. M., A. V. Panfilov, and F. U. Medvedeva. 1983. Instability of autowaves in excitable media associated with the phenomenon of critical curvature. *Biofizika.* 28:100–102.

Rushton, W. A. H. 1937. Initiation of the propagated disturbance. *Proc. R. Soc. Lond. B Biol. Sci.* 124:210–243.

Starobin, J. M., Y. I. Zilberter, E. M. Rusnak, and C. F. Starmer. 1995. Wavelet formation in excitable cardiac tissue: the role of wavefront-obstacle interactions in initiating high-frequency fibrillatory-like arrhythmias. *Biophys. J.* In press.

Toth, A., V. Gaspar, and K. Showalter. 1994. Signal transmission in chemical systems: propagation of chemical waves through capillary tubes. *J. Phys. Chem.* 98:522–531.

Tritton, D. J. 1977. Physical Fluid Dynamics. Van Nostrand Reinhold, Berkshire, England. 21–27.

Winfree, A. T. 1989. Electrical instability in cardiac muscle: phase singularities and rotors. *J. Theor. Biol.* 138:353–405.

Winfree, A. T. 1994. Electrical turbulence in three-dimensional heart muscle. *Science.* 266:1003–1006.

Zhabotinsky, A. M., M. D. Eager, and I. R. Epstein. 1993. Refraction and reflection of chemical waves. *Phys. Rev. Lett.* 71:526–1529.

Zykov, V. S. 1988. Simulations of Wave Processes in Excitable Media. Manchester University Press, Manchester.